THERMODYNAMIC CHARACTERIZATION OF MULTIPHASE NON-METALLIC INCLUSIONS IN RE-SULPHURISED STEEL GRADES

TERMODINAMIČNA KARAKTERIZACIJA VEČFAZNIH NEKOVINSKIH VKLJUČKOV V JEKLIH S POVIŠANIM ŽVEPLOM

Luka Krajnc[1], Primož Mrvar[2], Jožef Medved[2]

[1]Štore Steel, d. o. o., Železarska 3, 3220 Štore, Slovenia
[2]University of Ljubljana, Faculty of Natural Sciences and Engineering, Department of Materials and Metallurgy, Aškerčeva 12, 1000 Ljubljana, Slovenia
luka.krajnc@store-steel.si

Non-metallic inclusion engineering is one of the most important aspects in steelmaking today. There are several thermodynamic and kinetic tools available that help to form non-metallic inclusions of the desired size, distribution and composition in steel. The goal of this work was to study the thermodynamic conditions responsible for the formation of multiphase inclusions in re-sulphurised steel grades that are produced for the automotive industry. Nozzle clogging on the continuous casting machine and surface defects on rolled rods are problems typically attributed to non-metallic inclusions. Samples of the 30MnVS6 steel grade were taken at five different stages of ladle treatment. The samples were prepared for metallography and images of inclusions were taken using a SEM. Thermodynamic calculations were made using the Thermo-calc software for each sample and for multiple inclusions in order to determine which phases are the most stable at a given stage of the ladle treatment. It was found that high-melting-point calcium sulphide (CaS) and spinel ($MgO \cdot Al_2O_3$) inclusions and low-melting-point calcium aluminate ($12CaO \cdot 7Al_2O_3$) or calcium alumosilicate ($2CaO \cdot Al_2O_3 \cdot SiO_2$) inclusions are the most stable phases in current steelmaking practice.

Keywords: calcium modification, CaS formation, non-metallic inclusion engineering

Inženiring nekovinskih vključkov je danes med najpomembnejšimi vidiki v jeklarstvu. Obstaja več termodinamičnih in kinetičnih orodij, ki pomagajo pri tvorbi vključkov z želeno velikostjo, porazdelitvijo in sestavo jekla. Cilj tega dela je bila študija termodinamičnih razmer, ki so odgovorne za nastanek večfaznih vključkov v jeklih s povišanim žveplom, ki se uporabljajo v avtomobilski industriji. Mašenje izlivkov na napravi za kontinuirno ulivanje jekla in površinske napake na valjanih palicah sta dve težavi, ki se ju pripisuje nekovinskim vključkom. Vzorci jekla 30MnVS6 so bili vzeti pri petih različnih stopnjah procesa obdelave v ponovči peči. Vzorci so bili pripravljeni za metalografsko preiskavo. Posnetki vključkov so bili napravljeni z vrstičnim elektronskim mikroskopom. Termodinamični izračuni so bili narejeni s programsko opremo Thermo-calc za določitev najbolj stabilne faze pri posameznih stopnjah procesa v ponovči peči. Ugotovljeno je bilo, da so termodinamično najbolj stabilne faze pri sedanji praksi izdelave jekla kalcijevi sulfidi (CaS) in špinelni ($MgO \cdot Al_2O_3$) vključki z visokim tališčem in kalcijevi aluminati ($12CaO \cdot 7Al_2O_3$) ter kalcijevi alumosilikati ($2CaO \cdot Al_2O_3 \cdot SiO_2$) z nizkim tališčem.

Ključne besede: modifikacija s kalcijem, nastanek CaS, inženiring nekovinskih vključkov

1 INTRODUCTION

The production of clean steel is one of the most important aspects in the steelmaking of special steel grades today. Clean steel is not defined only as steel with a low total content of non-metallic inclusions, but also as steel with an engineered size, distribution and composition of these inclusions. This is especially true for the steel grades produced for the automotive industry, where sulphide inclusions are used to increase the machinability of steel[1]. A typical re-sulphurised steel

grade produced in large quantities nowadays is 30MnVS6; its standard chemical composition can be seen in **Table 1**.

This research focuses on the formation of multiphase non-metallic inclusions and looks at the thermodynamic conditions at different points of secondary steelmaking.

2 THERMODYNAMICS OF DEOXIDATION AND MODIFICATION OF INCLUSIONS

After oxygen rafination the steel has a high soluble oxygen concentration. In order to reduce it, elements with a high oxygen affinity (silicon, manganese and aluminium) are added. Deoxidation reactions and free-energy changes in the standard state are given in **Table 2**.[2]

Aluminium has the highest affinity for oxygen and therefore if its concentration in the melt is high enough, solid alumina inclusions are formed. On the other hand,

Table 1: Standard chemical composition of 30MnVS6 steel grade in mass fractions, *w*/%
Tabela 1: Standardna kemijska sestava jekla 30MnVS6 v masnih deležih, *w*/%

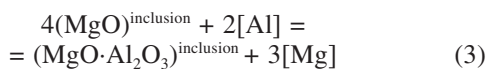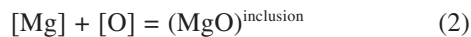| Element	C	Si	Mn	P	S	Cr	Mo	V	N
Min.	0.26	0.15	1.20	–	0.02	–	–	0.08	0.01
Max.	0.33	0.80	1.60	0.025	0.06	0.30	0.08	0.20	0.02

Table 2: Deoxidation reactions and free-energy changes in the standard state
Tabela 2: Reakcije dezoksidacije in spremembe prostih energij pri standardnih razmerah

Deoxidation reaction[2]	$\Delta G°$/(J/mol)
$[Si] + 2[O] = (SiO_2)_{(s)}$	$-594230 + 229.73·T$
$2[Al] + 3[O] = (Al_2O_3)_{(s)}$	$-1201860 + 323.22·T$
$[Mn] + [O] = (MnO)_{(s)}$	$-288120 + 128.26·T$

if the aluminium concentration is low a ternary system of inclusions MnO-SiO$_2$-Al$_2$O$_3$ is a result of a complex deoxidation. Kiessling[3] made an extensive research on this system and found that the properties of inclusions with a low melting point (MnO·SiO$_2$, 3MnO·Al$_2$O$_3$· 3SiO$_2$) are much more beneficial than those with a high melting point (Al$_2$O$_3$, SiO$_2$) since they are softer and can be more easily deformed[3]. Thermodynamic models[4,5] together with experimental and industrial trials[6–8] have been employed to study the system in detail. Kang and Lee[6] found that for $w(Mn) + w(Si) = 1$ %, a MnO/SiO$_2$ ratio in the range from 0.5 to 2 gives low melting temperatures, with the ratio of 1 giving the lowest and also the widest window for the alumina content of an inclusion, which is otherwise in the range from $w = 10$ % to $w = 20$ %.

With high aluminium concentrations in the steel, good thermodynamic conditions are met for the formation of the spinel MgO-Al$_2$O$_3$ phase[9]. According to Park et al.[10,11] there are two mechanisms for the formation of the MgO-Al$_2$O$_3$ phase. The first is the singular spinel formation route and the second is the crystallization that takes place on the solidification path of alumosilicate slag droplets. In our case the first is more likely, so the reactions governing this route are given:

$$2[Al] + 3(MgO)^{slag\ or\ refractory} = 3[Mg] + (Al_2O_3) \quad (1)$$

$$[Mg] + [O] = (MgO)^{inclusion} \quad (2)$$

$$4(MgO)^{inclusion} + 2[Al] = \\ = (MgO·Al_2O_3)^{inclusion} + 3[Mg] \quad (3)$$

Free-energy changes in the standard state for the Reactions 2 and 3 are given in **Table 3**.

Table 3: Free-energy changes in the standard state for Reactions 2 and 3
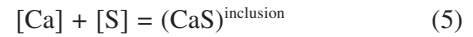**Tabela 3:** Spremembe prostih energij pri standardnih razmerah za reakciji 2 in 3

Reaction[11]	$\Delta G°$/(kJ/mol)
$[Mg] + [O] = (MgO)$	$-89.98 - 0.08194·T$
$4(MgO) + 2[Al] = \\ = (MgO·Al_2O_3) + 3[Mg]$	$-423.01 + 0.275·T$

Several mechanisms for the removal of the spinel phase have been discused[11–13]. Using a high basicity slag and a calcium treatment are the most successful. The latter has been investigated in great detail for the solid alumina modification. Both thermodynamic[14–20] and kinetic[21,22] fundamentals have been laid. With the addition of calcium, CaO-Al$_2$O$_3$ (CA) inclusions with a low

melting point are formed based on Reaction 4[23]; however, calcium also has a high affinity for sulphur, so a CaS inclusion can be formed based on Reaction 5:

$$x[Ca] + (1-2/3x)Al_2O_3 = (CaO)_x(Al_2O_3)_{1-x} + 2/3x[Al] \quad (4)$$

$$where\ 0 < x = 1;$$

$$[Ca] + [S] = (CaS)^{inclusion} \quad (5)$$

The CA phases formed are: CaO·6Al$_2$O$_3$ (CA$_6$), CaO·2Al$_2$O$_3$ (CA$_2$), CaO·Al$_2$O$_3$ (CA), 12CaO·7Al$_2$O$_3$ (C$_{12}$A$_7$), 3CaO·Al$_2$O$_3$ (C$_3$A)[24]. The phase with the lowest melting point is C$_{12}$A$_7$. The CA phase is also liquid at steelmaking temperatures[24]. They are formed according to the following reactions:

$$(CaO) + (Al_2O_3) = (CaO·Al_2O_3) \quad (6)$$

$$12(CaO) + 7(Al_2O_3) = (12CaO·7Al_2O_3) \quad (7)$$
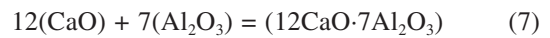
The free-energy changes in the standard state for the Reactions 5, 6 and 7 are given in **Table 4**.[25,26]

Table 4: Free-energy changes in the standard state for Reactions 5, 6 and 7
Tabela 4: Spremembe prostih energij pri standardnih razmerah za reakcije 5, 6 in 7

| Reaction[25,26]	$\Delta G°$/(J/mol)
$[Ca] + [S] = (CaS)$	$-542531 + 124.15·T$
$(CaO) + (Al_2O_3) = (CaO·Al_2O_3)$	$-19246 - 18·T$
$12(CaO) + 7(Al_2O_3) = \\ = (12CaO·7Al_2O_3)$	$+617977 - 612·T$

Both non-fully modified alumina inclusions and CaS inclusions can be the reason for nozzle clogging on the continuous casting machine. Janke et al.[27] made a thermodynamic model to improve the castability and confirmed it with practical results. Vermeulen et al.[28] made experiments to see how different refractories react with steel, slag and inclusions. Lamut et al.[29] found that the spinel-type inclusions (MgO,MnO)·Al$_2$O$_3$, CaS and non-fully-modified alumina inclusions (CaO·2Al$_2$O$_3$) are the main reasons for clogging.

3 EXPERIMENTAL

Samples of the re-sulphurised steel grade 30MnVS6 were taken at five different stages of ladle furnace treatment: after homogenization, before and after calcium addition, after sulphur addition and 20 min after sulphur addition. The samples were taken using the Sample-on-Line method or the Lollipop-sampling method, they are marked 1–5.

Chemical analyses were on the samples using optical emission spectroscopy with an instrument made by Spectro, LAVMC12A.

The samples were metallographically prepared and investigated using a scanning electron microscope JEOL JSM-6390 LV equipped with an EDS Inca X-sight module from Oxford Instruments.
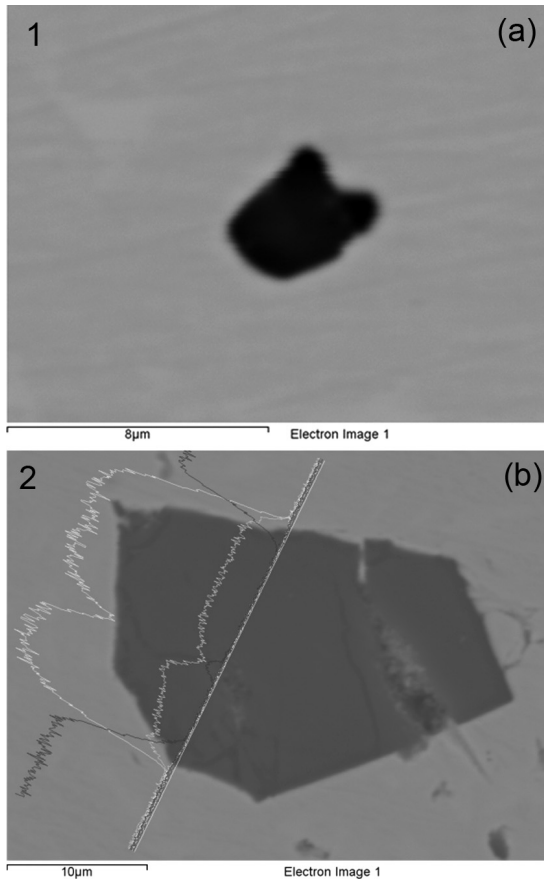
Figure 1: SEM images of inclusions: a) small alumina inclusion 1, b) large alumina inclusion 2
Slika 1: SEM-posnetka vključkov: a) majhen aluminatni vključek 1, b) velik aluminatni vključek 2
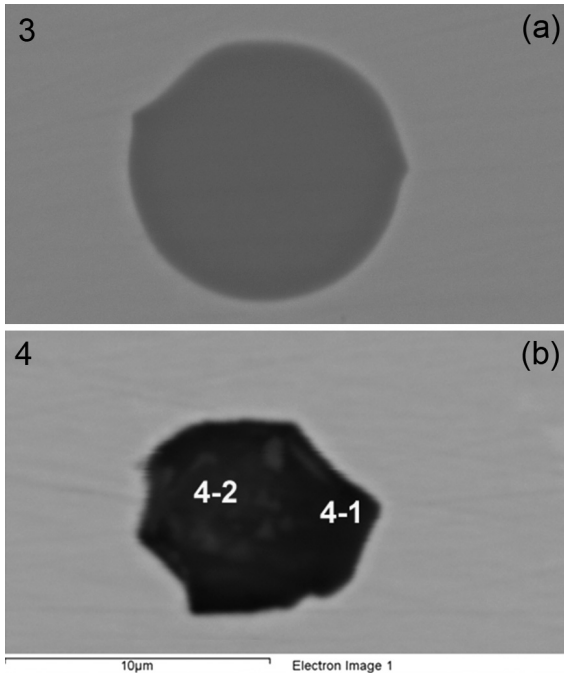
Figure 2: SEM images of inclusions: a) liquid single-phase inclusion 3, b) solid multiphase inclusion 4 from MnO-SiO_2-Al_2O_3 system
Slika 2: SEM-posnetka vključkov: a) tekoč enofazni vključek 3, b) trden večfazni vključek 4 iz sistema MnO-SiO_2-Al_2O_3

The methodology used when analysing the inclusions was as follows: the inclusion was found, different phases were identified using a line or a mapping analysis. Afterwards, a point analysis was made for each separate phase. The results obtained with the point analyses were then used for the thermodynamic calculation.

The thermodynamic analysis of the inclusions was performed with Thermo-Calc TCW5 software. The calculations were made using the SSUB3 and SLAG1 databases.

4 RESULTS

Two different types of inclusions were found in sample 1: solid alumina inclusions either with a low MgO content or with no MgO content and inclusions from the MnO-SiO_2-Al_2O_3 system, which are either solid or liquid. Examples can be seen in **Figures 1** and **2**.

The Fe content in the samples is due to the matrix, so it was disregarded in the thermodynamic calculations. The phase composition of different inclusions is shown in **Table 5**.

Table 5: Phase composition of inclusions 1, 2, 3 and 4
Tabela 5: Fazna sestava vključkov 1, 2, 3 in 4

Inclusion	Phase composition, w/%			
	Al_2O_3	SiO_2	MnO	MgO
1	88	0	0	12
2	100	0	0	0
3	12	44	39	0
4-1	32	40	28	0
4-2	72	22	6	0

At steelmaking temperatures the complex phases calculated using Thermo-calc software are presented in **Table 6**.
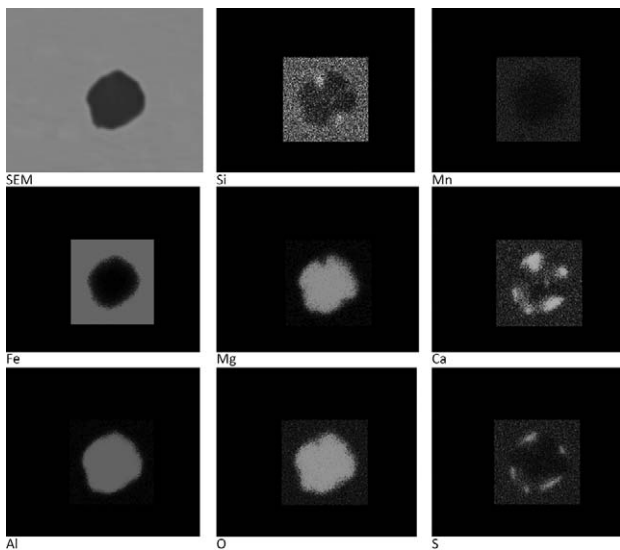
Table 6: Calculated phase composition of inclusions 1, 2, 3 and 4 at steelmaking temperatures
Tabela 6: Preračunana fazna sestava vključkov 1, 2, 3 in 4 pri temperaturah izdelave jekla

Inclusion	Phase composition, w/%					
	$MgO\cdot Al_2O_3$	Al_2O_3	SiO_2	$3Al_2O_3\cdot 2SiO_2$	$2MnO\cdot SiO_2$	$MnO\cdot 2Al_2O_3$
1	41	59	0	0	0	0
2	0	100	0	0	0	0
3	0	0	17	32	51	0
4-1	0	0	9	57	34	0
4-2	0	34	0	56	0	10

Liquid inclusions from the MnO-SiO_2-Al_2O_3 system are still present in sample 2. There are also solid spinel-type inclusions. A mapping analysis of such an inclusion was made and it can be seen in **Figure 3**. It is about 8 μm in diameter.

The calculated phase composition at steelmaking temperatures of the central part of this inclusion is shown in **Table 7**.

Figure 3: A mapping analysis of a spinel-type inclusion with the CaS and xCaO·yAl$_2$O$_3$·zSiO$_2$ phases
Slika 3: Ploskovna analiza špinelnega vključka s CaS in fazami xCaO·yAl$_2$O$_3$·zSiO$_2$
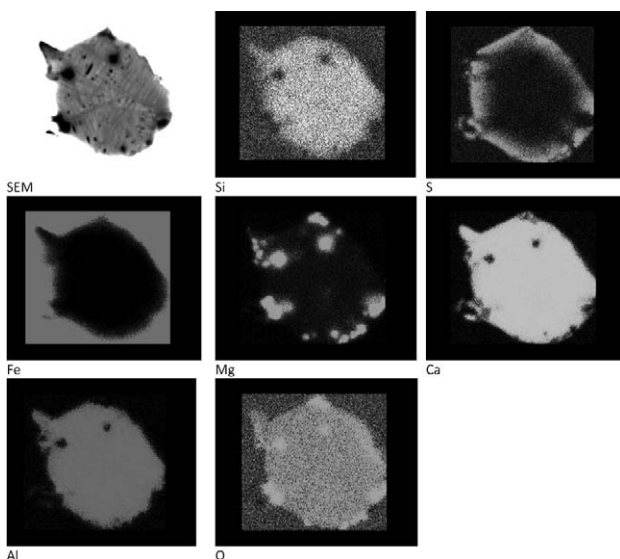
Table 7: Calculated phase composition of the central part of inclusion 5 at steelmaking temperatures
Tabela 7: Preračunana fazna sestava srednjega dela vključka 5 pri temperaturah izdelave jekla

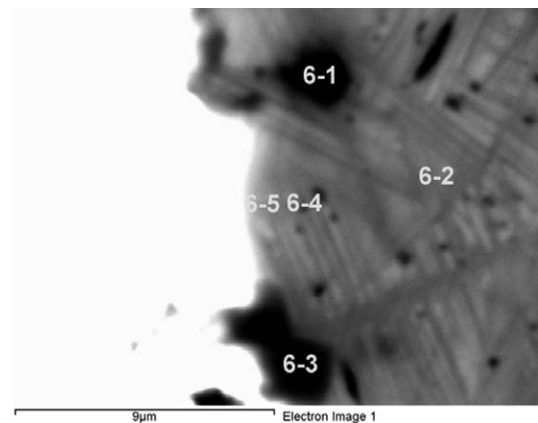|	Phase composition, w/%	
Inclusion	MgO·Al$_2$O$_3$	Al$_2$O$_3$
5	95	5

The inclusion analysed in sample 3 is the large multiphase macro inclusion number 6. It is about 25 μm in diameter. A mapping analysis is shown in **Figure 4**.

Phase compositions of different parts of inclusion 6 are shown in **Table 8**. A magnified SEM image on the right central part of the inclusion 6 is seen in **Figure 5**.

Figure 4: A mapping analysis of a large multiphase inclusion 6
Slika 4: Ploskovna analiza večfaznega vključka 6

Figure 5: A magnified SEM image of inclusion 6
Slika 5: Povečan del vključka 6 (SEM)

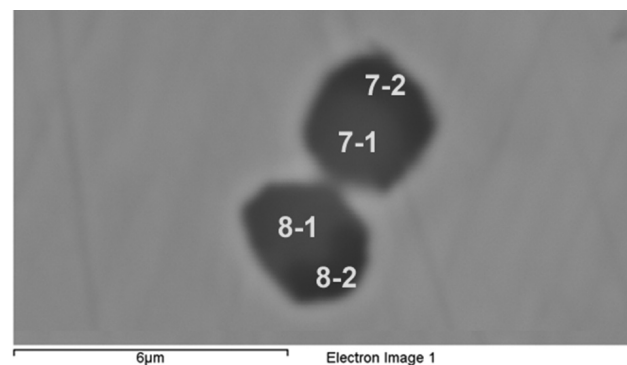**Table 8:** Calculated phase composition of different parts of inclusion 6 at steelmaking temperatures
Tabela 8: Preračunana fazna sestava različnih delov vključka 6 pri temperaturah izdelave jekla

Inclu-sion	Phase composition, w/%					
	12CaO·7Al$_2$O$_3$	CaS	2CaO·Al$_2$O$_3$·SiO$_2$	MgO	2CaO·SiO$_2$	MgO·Al$_2$O$_3$
6-1	7	4	15	66	0	8
6-2	58	0	18	4	20	0
6-3	15	1	13	71	0	0
6-4	57	1	25	4	13	0
6-5	47	7	42	4	0	0

Table 9: Calculated phase composition of different parts of inclusions 7 and 8 at steelmaking temperatures
Tabela 9: Preračunana fazna sestava različnih delov vključkov 7 in 8 pri temperaturah izdelave jekla
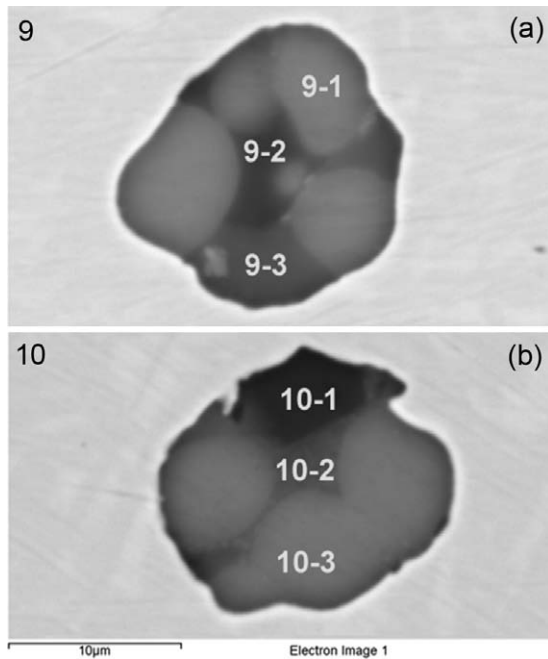
Inclu-sion	Phase composition, w/%							
	12CaO·7Al$_2$O$_3$	CaS	2CaO·Al$_2$O$_3$·SiO$_2$	MgO	CaO	2CaO·SiO$_2$	CaO·2Al$_2$O$_3$	MgO·Al$_2$O$_3$
7-1	12	74	0	0	11	3	0	0
7-2	59	18	0	3	1	19	0	0
8-1	13	82	1	1	0	3	0	0
8-2	4	5	46	0	0	0	22	23

Figure 6: SEM image of two two-phase inclusions
Slika 6: SEM-posnetek dveh dvofaznih vključkov

Figure 7: SEM images of inclusions: a) multiphase inclusion 9 found in sample 4, b) multiphase inclusion 10 found in sample 5
Slika 7: SEM-posnetka vključkov: a) večfazni vključek 9 iz vzorca 4, b) večfazni vključek 10 iz vzorca 5

Table 10: Calculated phase composition of different parts of inclusions 9 and 10 at steelmaking temperatures
Tabela 10: Preračunana fazna sestava različnih delov vključkov 9 in 10 pri temperaturah izdelave jekla

Inclu-sion	Phase composition, w/%						
	$12CaO \cdot 7Al_2O_3$	CaS	$2CaO \cdot Al_2O_3 \cdot SiO_2$	MgO	$2CaO \cdot SiO_2$	$MgO \cdot Al_2O_3$	Al_2O_3
9-1	0	100	0	0	0	0	0
9-2	0	13	0	0	0	83	4
9-3	26	0	69	3	0	2	0
10-1	0	0	0	0	0	100	0
10-2	45	0	34	5	16	0	0
10-3	0	100	0	0	0	0	0

Table 11: Free-energy values in the standard state for the most stable phases in samples 4 and 5
Tabela 11: Izračunane proste energije pri standardnih razmerah za najbolj stabilne faze v vzorcih 4 in 5

Reaction	ΔG at 1600 °C
$[Ca] + [S] = (CaS)$	–309998
$(CaO) + (Al_2O_3) = (CaO \cdot Al_2O_3)$	–52960
$12(CaO) + 7(Al_2O_3) = (12CaO \cdot 7Al_2O_3)$	–528299
$[Mg] + [O] = (MgO)$	–243454
$4(MgO) + 2[Al] = (MgO \cdot Al_2O_3) + 3[Mg]$	+92065

The second two inclusions analysed are two-phase inclusions; they can be seen in **Figure 6**. Their calculated phase composition at steelmaking temperatures is shown in **Table 9**.

In samples 4 and 5 there are examples of liquid inclusions from the $MnO-SiO_2-Al_2O_3-CaO$ system. Predo-

minantly, however, the multiphase inclusions shown in **Figure 7** were found.

The calculated phase composition at steelmaking temperatures of the two inclusions is shown in **Table 10**.

The free energies at standard state calculated at 1600 °C for the most stable phases of the inclusions found in samples 4 and 5 are given in **Table 11**.

5 DISCUSSION

In the first sample, pure alumina inclusions were found, an example is inclusion 2 and there is already evidence of the formation of a spinel phase. It can be seen in alumina inclusion 1, where there is enough magnesium to contribute to 41 % of the spinel phase calculated in equilibrium conditions. It is also evident that the higher concentration of alumina in the inclusions from the $MnO-SiO_2-Al_2O_3$ system the higher is their melting point. Inclusion 3 with a low alumina content is liquid at steelmaking temperatures and inclusion 4 with a high alumina content is solid.

In the second sample the MgO content of the investigated inclusions has increased almost to the equilibrium spinel state, as shown in **Table 7**. Inclusion 5 is a typical representative. Already there are a phase from the $CaO-Al_2O_3-SiO_2$ system and a CaS phase forming at the edge of the inclusion. The solid $MgO \cdot Al_2O_3$ acts as a nucleus for these phases.

The inclusion 6 in sample 3 is made out of a predominantly liquid matrix of two phases: $12CaO-7Al_2O_3$ and $2CaO-Al_2O_3-SiO_2$. There are several examples of pure MgO phases, they have been formed according to Reaction 2, and because they are solid at steelmaking temperatures they have been incorporated into the liquid matrix. It is evident that the sulphur concentration increases towards the edge of the inclusion. This is in agreement with the literature[22,23]. The sulphur concentration in steel is at this moment insufficient to form a stable CaS phase. The inclusions 7 and 8 in this steel sample are two-phase inclusions, the lighter shade is a mostly CaS phase and the darker shade is either mostly spinel ($MgO \cdot Al_2O_3$) phase or mostly liquid $CaO \cdot Al_2O_3 \cdot SiO_2$ phase. They are about 2 μm in size.

In the last two samples mostly one kind of multiphase inclusion was found. They are composed of three phases. The first one is the spinel ($MgO \cdot Al_2O_3$) phase, this is the darkest. The lightest is the CaS phase. The middle shade phase is a $CaO-Al_2O_3-SiO_2$ system phase. These are liquid at steelmaking temperatures, whereas the spinel and CaS are solid.

The spinel phase formed in the early stages of the ladle furnace treatment, the mechanisms for its formation have been explained[10,11]. After the addition of calcium, the modification of alumina, spinel type and $MnO-SiO_2-Al_2O_3$ system based inclusions began. The alumina modification was successful and the liquid CA inclusions were formed. The calcium reduced the manganese and

also liquid $CaO-Al_2O_3-SiO_2$ system inclusions were formed. In general, calcium was unable to modify the spinel-type inclusions. In a previous study[30], unmodified spinel inclusions surrounded by liquid CA were found, but the sulphur concentration was lower and they were eventually modified. In the case of a higher sulphur concentration, calcium's ability to modify the alumina and spinel-type inclusions is greatly inhibited and mostly the CaS phase is formed. Previous studies[11–13] that reported the modification of spinel-type inclusions were dealing with low sulphur concentrations.

According to the thermodynamic calculations the CaS and spinel phases are very stable in sample 5 and also the low-melting-point CA and $CaO-Al_2O_3-SiO_2$ system based phases are stable, only a small amount of MgO was detected, which is probably due to the measurement technique. According to **Table 11** these phases also have the lowest free energies at 1600 °C, only spinel inclusions do not have a low free energy at this point in the process, but they have been created earlier, at the beginning of ladle furnace treatment.

Because these types of inclusions (9, 10) are mostly solid (CaS, spinel), only a small part being liquid ($12CaO·7Al_2O_3$, $2CaO·Al_2O_3·SiO_2$), they do not have the tendency to combine and form larger inclusions that float to the slag more easily. They therefore have a negative effect on castability; studies[29] have shown that phases found in this type of inclusions are also found on the submerged entry nozzles on the continuous casting machine and cause nozzle clogging.

It should be noted that some large exogenous inclusions were also found, they act as nuclei for smaller indigenous inclusions, but they were not the focus of this research. Because of their large size they are quickly removed to the slag.

6 CONCLUSIONS

Thermodynamic conditions for the formation of multiphase non-metallic inclusions have been investigated. Figures showing the typical inclusions have been presented for each sample taken. Based on the results, the following conclusions can be drawn:

- High aluminium concentrations after tapping decrease the ability to form liquid $MnO-SiO_2-Al_2O_3$ system based inclusions and increase the ability for spinel-type inclusions to be formed.
- Calcium modifies alumina, alumosilica and $MnO-SiO_2-Al_2O_3$ system based inclusions.
- In the case of a high sulphur concentration the calcium does not modify the spinel ($MgO·Al_2O_3$) type inclusions
- Multiphase type of inclusions CaS, spinel ($MgO·Al_2O_3$) and $12CaO·7Al_2O_3$, $2CaO·Al_2O_3·SiO_2$) are detrimental to the castability of the steel.

7 REFERENCES

[1] L. Holappa, M. Hämäläinen, M. Liukkonen, M. Lind, Thermodynamic Examination of Inclusion Modification and Precipitation from Calcium Treatment to Solidified Steel, Ironmaking and Steelmaking, 30 (**2003**) 2, 111–116

[2] G. Pierson, B. Sander, Amélioration des Performances de Coupe des Aciers Doux de Décolletage par Maitrise de leur Contenu Inclusionnaire, EUR16020, 1995

[3] R. Kiessling, Non-metallic Inclusions in Steel, The Metals Society, London 1968, 10, 17, 44, 52

[4] I. H. Jung, S. A. Decterov, A. D. Pelton, A Thermodynamic Model for Deoxidation Equilibria in Steel, Metallurgical and Materials Transactions B, 35 (**2004**), 493–507

[5] I. H. Jung, S. A. Decterov, A. D. Pelton, Computer Applications of Thermodynamic Databases to Inclusion Engineering, ISIJ International, 44 (**2004**) 3, 527–536

[6] Y. B. Kang, H. G. Lee, Inclusions Chemistry for Mn/Si Deoxidized Steels: Thermodynamic Predictions and Experimental Confirmations, ISIJ International, 44 (**2004**) 6, 1006–1015

[7] X. Zhang, H. Roelofs, S. Lemgen, U. Urlau, S. V. Subramanian, Application of Thermodynamic Model for Inclusion Control in Steelmaking to Improve the Machinability of Low Carbon Free Cutting Steels, Steel Research Int., 75 (**2004**) 5, 314–321

[8] Y. Payandeh, M. Soltanieh, Oxide Inclusions at Different Steps of Steel Production, Journal of Iron and Steel Research International, 14 (**2007**) 5, 39–46

[9] D. Steiner Petrovič, B. Arh, F. Tehovnik, M. Pirnat, Magnesium Non-metallic Inclusions in Non-oriented Electrical Steel Sheets, ISIJ International, 51 (**2011**) 12, 2069–2075

[10] J. H. Park, Formation Mechanism of Spinel-Type Inclusions in High-Alloyed Stainless Steel Melts, Metallurgical and Materials Transactions B, 38 (**2007**), 657–663

[11] J. H. Park, H. Todoroki, Control of $MgO-Al_2O_3$ Spinel Inclusions in Stainless Steels, ISIJ International, 50 (**2010**) 10, 1333–1346

[12] S. F. Yang, J. S. Li, Z. F. Wang, J. Li, L. Lin, Modification of $MgO-Al_2O_3$ Spinel Inclusions in Al-Killed Steel by Ca-Treatment, International Journal of Minerals, Metallurgy and Materials, 18 (**2011**), 18–23

[13] M. Jiang, X. Wang, B. Chen, W. Wang, Laboratory Study on Evolution Mechanisms of Non-metallic Inclusions in High Strength Alloyed Steel Refined by High Basicity Slag, ISIJ International, 50 (**2004**) 1, 95–104

[14] V. Prešern, B. Koroušić, J. W. Hastie, Thermodynamic Conditions for Inclusions Modification in Calcium Treated Steel, Steel Research, 62 (**1991**) 7, 289–295

[15] F. Tehovnik, B. Koroušić, V. Prešern, Optimization of the Modification of Nonmetallic Inclusions in Steel with CaSi Wire Injection, Kovine, Zlitine, Tehnologije, 26 (**1992**) 1–2, 125–130

[16] J. C. S. Pires, A. Garcia, Modification of Oxide Inclusions Present in Aluminium-Killed Low Carbon Steel by Addition of Calcium, Rem: Rev. Esc. Minas, 57 (**2004**) 3, 183–189

[17] S. Abdelaziz, G. Megahed, I. El-Mahallawi, H. Ahmed, Control of Ca addition for improved cleanness of low C, Al killed steel, Ironmaking and Steelmaking, 39 (**2009**) 6, 432–441

[18] Y. Higuchi, M. Numata, S. Fukagawa, K. Shinme, Inclusion Modification by Calcium Treatment, ISIJ International, 36 (**1996**), 151–154

[19] C. E. Cicutti, J. Madras, J. C. Gonzales, Control O Microinclusions in Calcium Treated Aluminium Killed Steels, Ironmaking and Steelmaking, 24 (**1997**) 2, 155–159

[20] Y. Kusano, Y. Kawauchi, M. Wajima, K. Sugawara, M. Yoshida, H. Hayashi, Calcium Treatment Technologies for Special Steel Bars and Wire Rods, ISIJ International, 36 (**1996**), 77–80

[21] D. Z. Lu, G. A. Irons, W. K. Lu, Kinetics and Mechanisms of Calcium Dissolution and Modification of Oxide and Sulphide Inclusions in Steel, Ironmaking and Steelmaking, 21 (**1994**) 5, 362–371

[22] G. Ye, P. Jönsson, T. Lund, Thermodynamics and Kinetics of the Modification of Al2O3 Inclusions, ISIJ International, 36 (**1996**), 105–108

[23] S. K. Choudhary, A. Ghosh, Thermodynamic Evaluation of Formation of Oxide-Sulfide Duplex Inclusions in Steel, ISIJ International, 48 (**2008**) 11, 1552–1559

[24] Schlackenatlas, Slag Atlas, Verlag Stahleisen, Düsseldorf 1981, 39

[25] O. Kubaschewski, C. B. Alcock, P. J. Spenscer, Materials Chemistry, 6th ed., Pergamon Press, Oxford 1993, 619

[26] R. H. Rein, J. Chipman, Trans. Metall. Soc. AIME, 233 (**1965**), 415

[27] D. Janke, Z. Ma, P. Valentin, A. Heinen, Improvement of Castability and Quality of Continuously Cast Steel, ISIJ International, 40 (**2000**) 1, 31–39

[28] Y. Vermeulen, B. Coletti, B. Blanpain, P. Wollants, J. Vleugels, Material Evaluation to Prevent Nozzle Clogging during Continuous Casting of Al Killed Steels, ISIJ International, 42 (**2002**) 11, 1234–1240

[29] J. Lamut, J. Falkus, B. Jurjovec, M. Knap, Influence of Inclusions Modification on Nozzle Clogging, Archives of Metallurgy and Materials, 57 (**2012**) 1, 319–324

[30] L. Krajnc, G. Klančnik, P. Mrvar, J. Medved, Thermodynamic analysis of the Formation of Non-metallic Inclusions during the Production of C45 Steel, Mater. Tehnol., 46 (**2012**) 4, 361–368